IEEE Access
Multidisciplinary | Rapid Review | Open Access Journal

Received June 29, 2020, accepted July 8, 2020, date of publication July 14, 2020, date of current version July 28, 2020.

Digital Object Identifier 10.1109/ACCESS.2020.3009089

Observer Based Sliding Mode Control for Hydraulic Driven Barrel Servo System With Unknown Dynamics

QUAN ZOU
School of Mechanical Engineering, Nanjing University of Science and Technology, Nanjing 210094, China
e-mail: zouquan101@163.com

ABSTRACT The position tracking control of a barrel system driven by a two-stage hydraulic cylinder with long transmission lines was addressed in this paper. First, an active balancing system was designed to balance the gravitational torque which may deteriorate the performance of the barrel control system. The active balancing system is totally isolated from the barrel control system; thus the dynamics of the barrel servo system is significantly simplified. The effects of the long transmission lines were also considered during the modeling of the barrel servo system. In order to exactly estimate the unmeasured states and the mechanical disturbance, an extended state observer was designed by employing the Levant's Differentiator, thus the estimation errors would converge to zero exponentially. Then, based on the estimated signals, the barrel system was transformed into the pure integration chain form, thus the sliding mode technology can be directly utilized. After that, a sliding mode controller is designed to make the position output of the barrel to track different motion trajectories as close as possible in the presence of model uncertainty and unknown dynamics. The closed loop system was proven to be asymptotical stable in the sense of Lyapunov theory. Three different motion trajectories were tested to verify the effectiveness of the proposed controller.

INDEX TERMS Barrel servo system, electrohydraulic servo system, sliding mode control, state estimation, unknown dynamics.

I. INTRODUCTION

Barrel servo system is a key component of modern pipe weapons since the combat effectiveness of the whole weapon system significantly depends on the control performance of the barrel system. Typically, there are two types of barrel servo system, namely, motor driven barrel servo system and hydraulic driven barrel servo system. The hydraulic driven barrel servo system is widely used in modern pipe weapons due to its high stiffness, high response and high load capability. The gravitational center of the barrel system is usually not aligned with the trunnion due to the structure feature and the space limitation, thus the unbalanced gravitational torque appears. Moreover, the unbalanced gravitational torque is function of the barrel angle, thus it is time-varying during the motion of the barrel. The time-varying unbalance gravitational torque can significantly deteriorate the control performance of the barrel servo system [1], [2]. To overcome this problem, passive balancing and active balancing are the most commonly used methods [2], [3]. In the passive balancing system, an inertia mass is usually used as the clump weight to make gravitational center aligned with the trunnion, thus the whole system is unwieldy and more energy is needed during the motion. In the active balancing system, the balancing torque is generated by another actuator, thus the whole system is much more light and energy-efficient. Hence, the active balancing system is widely used in modern pipe weapon systems. A hydraulic cylinder with three chambers was used as the balancing system in [4], thus the driving forces of the actuator is significantly reduced. Similarly, the three chambered hydraulic cylinder was also employed in the barrel servo system in [2]. The main disadvantage of this balancing strategy is that the three chambered hydraulic cylinder is expensive and the dynamics of the whole system is complicated. Another commonly used method in the hydraulic balancing system is the usage of the balance valve. However, the balance valve usually produces large pressure drop, which make the system inefficient. In this paper, a simple but effective hydraulic

The associate editor coordinating the review of this manuscript and approving it for publication was Yanbo Chen.

balancing system was designed, which will be explained in detail in section 2.1.

Apart from the unbalanced torque, the barrel servo system studied in this paper is essentially a strong nonlinear system subjected to unknown external mechanical disturbance and large hydraulic parameter variations. The nonlinearity is mainly caused by the pressure-flow characteristic of the servo valve, nonlinear frictions and the structure of the system. Recently, several advanced control methods had been developed for the position tracking control of the electro-hydraulic system (EHS), such as passivity-based control [5], [6], linearization-based control [7], [8], back-stepping based control [9], [10], adaptive robust control [11], [12] and so on. Sliding mode control (SMC) was also widely used in EHS for its fast response, simplicity and robust [2], [9], [10]. Theoretically, SMC is robust only to matched disturbance (including matched model uncertainties). Unfortunately, the mechanical disturbances in EHS is mismatched, thus SMC cannot be directly used in position control of EHS. To overcome this problem, the back-stepping based SMC was proposed for the position tracking control of EHS in [9] and [10], and excellent results had been obtained. However, the control law is extremely complicated due to the differentiating of the virtual control signal in each step, which is well-known as ''explosion of term'' problem. The multiple-surface based sliding mode control [13], [14] is essentially the same as the back-stepping based sliding mode control, in which the ''explosion of term'' problem also exits. The dynamic surface technology [15] can be used to calculate the derivative of the virtual control signal in each step, thus the back-stepping based control law is significantly simplified, but this usually leads to slower response of the closed loop system due to the extra dynamics of the controller. Generally speaking, the bound of the lumped disturbance should be known to design the switching control law of SMC, but this bound is not always known in practical applications due to the complicated dynamics of the controlled plant. Disturbance observer (DOB) based sliding mode control were developed for system with matched and mismatched disturbance in [16] and [17], in which the bound of the disturbance was not needed and the switching gain was only needed to be greater than the bound of the estimation error, thus the chattering phenomenon was significantly reduced. However, good estimation performance can be obtained only when the disturbance is constant or slow-varying, which is difficult to fulfill in practical applications. Another obstacle for the real applications of SMC is the well-known chattering phenomenon that caused by sensor delays, unmolded dynamics, non-ideal switching and so on [18]. In order to reduce or even eliminate the chattering phenomenon, several methods, such as boundary layer, continuous approximation function, soft computing based optimization and high order sliding mode based control had been proposed [16], [18]. The effectiveness of the above mentioned methods for chattering attenuation have already proved in practical applications.

Another difficulty of the position tracking control of EHS is the unmeasured states. A high gain observer (HGO) was designed to estimate the unmeasured states of an electro hydraulic loading system [19], and the HGO was proven to be exponentially stable. The HGO was used to estimate the full-state of an active suspension system in [20], and simulations were performed to verify the effectiveness of the HGO. However, HGO is not robust enough to model uncertainties and external disturbances, thus, the performance of the HGO based control would degrade significantly when large model uncertainty or disturbance appears. Moreover, HGO can only estimate the unmeasured states. To attenuate the effect of model uncertainty and disturbance, an unknown dynamic estimator (UDE) was designed to estimate the unknown lumped disturbance of the EHS in [21], and meanwhile, the Levant's Differentiator [22] was employed to obtain the higher order derivatives of the output signal. However, the estimation error always exists due to the nonzero time constant of the low-pass filter. In order to simultaneously estimate the unmeasured states and unknown disturbance of the EHS, extended state observer (ESO) was firstly employed by Yao *et al.* in [23], and the effectiveness of the ESO was verified though extensive experiments. The ESO was also employed to estimate the full states and unknown disturbance of the EHS in [24], although the mismatched disturbance was temporarily ignored during the design of ESO, the ESO is proven to be robust to the mismatched disturbance. Theoretically, the estimation errors of the traditional linear ESO can be effectively reduced by tuning the observer bandwidth, however, the estimation errors always exist when the disturbance is not exactly known [25], [26] and too large observer bandwidth would lead to peak phenomenon which is not desired in practical applications.

In this paper, motived by the above discussions, a novel nonlinear ESO was designed to simultaneously estimate the unmeasured states and unknown disturbance of the barrel system by employing the Levant's Differentiator. Thus, the estimation errors would converge to zero exponentially, which means that the estimated states would converge to their true values. Then, based on the estimated signals, the barrel system was transformed into the pure integration chain form. Hence, the sliding mode control technology can be directly used. To attenuate the hydraulic uncertainties, a sliding mode controller was designed as the position tracking controller based on the new state variables. The closed loop system was proven to be exponentially stable in the sense of Lyapunov theory.

II. DYNAMIC MODELS AND PROBLEM FORMULATION

A. DECRIPSION OF THE ACTIVE BALANCING SYSTEM

In this section, a simple but effective hydraulic active balancing system is designed. As shown in Figure 1, the active balancing system is mainly comprised of three accumulators and a two-stage hydraulic cylinder whose structure is the same as the actuator of the barrel servo system.

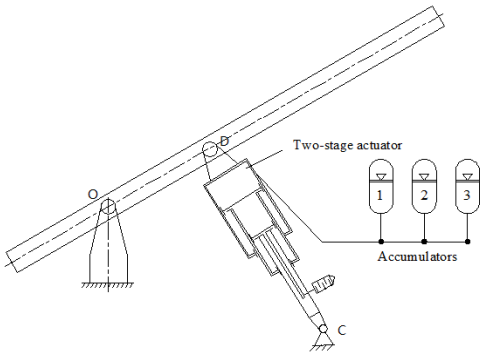

FIGURE 1. Schematic diagram of the active balancing system.

TABLE 1. Main parameters of the active balancing system.

Accumulator No.	Nominal volume(L)	Working volume(L)	Gas pressure (Mpa)
1	3.85	1.16	6.69
2	2.23	0.46	4.61
3	0.88	0.30	2.32

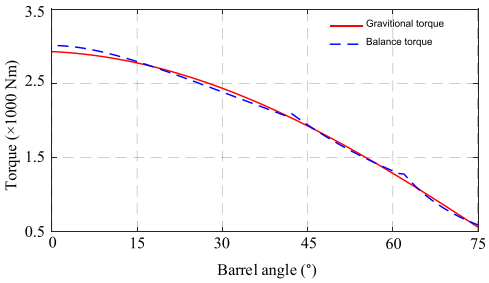

FIGURE 2. Curves of gravitational torques and balance torques.

The three accumulators are placed in parallel, and the gas pressure of each accumulator is carefully designed such that each of them works mainly at specific barrel angle ranges. The gravitational torques within the angle 0-40 degrees, 40-60 degrees and 60-75 degrees are mainly balanced by one of the three accumulators. The main parameters of the three accumulators are given in Table 1. The curves of the gravitational torque and the balance torque provided by the active balancing system are depicted in Figure 2. As can be seen, although not totally compensated, the unbalanced torques are kept at small arrange throughout the whole working area. It is also should be noted that the active balancing system is totally isolated from the barrel servo system, which make the dynamics of the barrel servo system significantly simplified.

B. DYNAMICS OF THE BARREL SERVO SYSTEM

The diagram of the barrel servo system is given in Figure 3. As can be seen, the structure and the placement of the actuator are the same as that of the active balancing system, thus the synchronous of the two actuators are guaranteed physically.

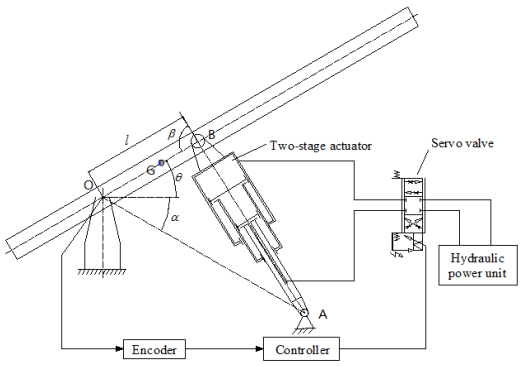

FIGURE 3. Diagram of the barrel servo system.

By using the Newton's Second Law, the mechanical dynamics of the barrel system can be given as

$$J\ddot{\theta} + B\dot{\theta} + T_d = Fl\sin\beta \tag{1}$$

where J is the equivalent moment of inertia; B is the equivalent viscous damping coefficient; T_d is the equivalent load torque including the unbalanced gravitational torques, external disturbances, nonlinear frictions and other unmolded dynamics. F is the driving force provided by the actuator, which can be given as

$$F = P_{1m}A_1 - P_{2m}A_2 \tag{2}$$

where P_{1m}, P_{2m}, A_1 and A_2 are the chamber pressures and the effective areas of the actuator, respectively.

Generally speaking, the dynamics of the servo valve should be considered when the response of the servo valve is not far greater than that of the controlled system. However, the sensing system of the valve spool displacement makes the servo valve very complicated and very limited control performance improvements are obtained. Moreover, a high response servo valve is used in the studied barrel servo system, thus it is reasonable to assume that the spool displacement is directly proportional to the control voltage applied to the servo valve, that is,

$$x_v = k_{sv}u \tag{3}$$

where x_v is the spool displacement of the servo valve, k_{sv} is the servo valve gain, and u is the control input voltages. In view of (3), it can be concluded that the sign of x_v is equivalent to that of u. Hence, the flow rate of the servo valve can be described as

$$Q_1 = s_s(u)k_q u\sqrt{P_s - P_1} + s_s(-u)k_q u\sqrt{P_1 - P_r} \tag{4}$$

$$Q_2 = s_s(u)k_q u\sqrt{P_2 - P_r} + s_s(-u)k_q u\sqrt{P_s - P_2} \tag{5}$$

where P_1 and P_2 are the pressures at port A and port B of the servo valve, respectively; P_s is the supply pressure; P_r is the returned pressure; k_q is the servo valve flow gain; and $s_s(u) = \begin{cases} 1, & u \geq 0 \\ 0, & u < 0 \end{cases}$.

Typically, the servo valve should be connected directly to the hydraulic cylinder to increase the stiffness and reduce the

parameter uncertainty of the controlled system. However, the servo valve cannot be directly connected to the actuator due to the imitated mounting space in the studied barrel system; thus long transmission lines are introduced to connect the servo valve and the actuator. Although the dynamics of the long transmission line is very complicated, it can well be approximated by a stable transfer function with time delay [28], i.e.,

$$P_{1m} = \frac{\psi(s+a)}{(s+b)} e^{-T_D s} P_1 = H_1(s) P_1 \tag{6}$$

$$P_{2m} = \frac{\psi(s+a)}{(s+b)} e^{-T_D s} P_2 = H_1(s) P_2 \tag{7}$$

where ψ is a constant that is determined by the structure of the pipe; the time delay constant T_D is determined by $T_D = L_m/C_{sd}$, in which L_m is the length of the pipe and C_{sd} is the speed of sound [28], [29].

Suppose that the external leakage of the actuator is zero, then the pressure dynamics of the actuator can be given as

$$\dot{P}_{1m} = \frac{\beta_e}{v_1}(Q_1 - A_1\dot{x}_A - C_i(P_{1m} - P_{2m})) \tag{8}$$

$$\dot{P}_{2m} = \frac{\beta_e}{v_2}(-Q_2 + A_2\dot{x}_A + C_i(P_{1m} - P_{2m})) \tag{9}$$

where v_1 and v_2 are the total control volumes including the volumes of the two actuator chambers and the long transmission lines; C_i is the internal leakage coefficient of the actuator; β_e s the modulus of the hydraulic oil; x_A is the displacement of the actuator rod.

If the state variables are defined as $x = [x_1, x_2, x_3]^T$, where $x_1 = \theta$, $x_2 = \dot{\theta}$ and $x_3 = (P_{1m}A_1 - P_{2m}A_2)/J$. Then the dynamics of the barrel servo system can be described in the state space form as follows.

$$\begin{cases} \dot{x}_1 = x_2 \\ \dot{x}_2 = ax_3 + d_1(t) \\ \dot{x}_3 = g(x,u)u - f(x,t)(P_1 - P_2) + d_2(x,t) \\ y = x_1 \end{cases} \tag{10}$$

where $a = l\sin\beta$, $d_1 = -(B + T_d)/J, f(x,t) = \frac{\beta_e}{J}(\frac{A_1}{v_1} + \frac{A_2}{v_2})C_iH_1$, $d_2(x,t) = -(\frac{\beta_e A_1^2}{Jv_1} + \frac{\beta_e A_2^2}{Jv_2})\dot{x}_A$, $g(x,u) = \frac{\beta_e}{J}(\frac{A_1R_1}{v_1} + \frac{A_2R_2}{v_2})$, in which $R_1 = s_s(u)k_q\sqrt{P_s - P_1} + s_s(-u)k_q\sqrt{P_1 - P_r}$, $R_2 = s_s(u)k_q\sqrt{P_2 - P_r} + s_s(-u)k_q\sqrt{P_s - P_2}$.

Without loss of generality, the following practical assumptions are made before the controller design.

Assumption 1: The unknown external disturbance d_1 *and* d_2 are bounded, *i. e.*, $|d_1| < \infty$, $|d_2| < \infty$. d_1 is differentiable and has a bounded derivative, i.e., $|\dot{d}_1| < \delta$, where δ is a known constant.

Assumption 2: Under normal working situations, the pressures P_1 and P_2 are both bounded by the supply P_s and return pressure P_r, which is about zero, i.e., $0 \approx P_r < P_1 < P_s, 0 \approx P_r < P_2 < P_s$. Thus, the chamber pressures of the actuator are also bounded by P_s and P_r, i.e., $0 \approx P_r < P_{1\mathrm{m}} < P_s$, $0 \approx P_r < P_{2\mathrm{m}} < P_s$.

Let x_d be the desired motion trajectory, and x_d is known and bounded up to the third order derivatives, i.e., $|x_d| + |\dot{x}_d| + |\ddot{x}_d| + |\dddot{x}_d| < \infty$. The objective in this paper is to synthesize a bounded control signal u such that the position tacking error is as small as possible in the presence of external disturbances and model uncertainties.

III. POSITION TRACKING CONTROLLER DESIGN

In view of (10), the mechanical disturbance d_1 is mismatched, thus the sliding mode control cannot be directly used. As discussed in section 1, the backstepping-based or multi-surface-based control is very complicated due to the "*explosion of term*" problem. Hence, the goal of this section is to design a sliding mode controller without using back-stepping or multi-surface.

A. DESIGN MODEL OF THE BARREL SERVO SYSTEM

In order to use the SMC technology directly, define a set of new state variables as follows

$$\begin{cases} \xi_1 = x_1 \\ \xi_2 = x_2 \\ \xi_3 = ax_3 + d_1(t) \end{cases} \tag{11}$$

Thus, the barrel servo system (10) can be rewritten as

$$\begin{cases} \dot{\xi}_1 = \xi_2 \\ \dot{\xi}_2 = \xi_3 \\ \dot{\xi}_3 = \phi_1 u - \phi_2(P_1 - P_2) + d \\ y = \xi_1 \end{cases} \tag{12}$$

where

$$\phi_1 = \frac{\beta_e}{J}(\frac{A_1R_1}{v_1} + \frac{A_2R_2}{v_2})l\sin\beta,$$

$$\phi_2 = \frac{1}{J}(\frac{\beta_e A_1}{v_1} + \frac{\beta_e A_2}{v_2})C_iH_1 l\sin\beta,$$

$$d(x,t) = -(\frac{\beta_e A_1^2}{Jv_1} + \frac{\beta_e A_2^2}{Jv_2})\dot{x}_A l\sin\beta + \dot{d}_1(t).$$

Note that the pressures P_1 and P_2 are both bounded, thus R_1 and R_2 are also bounded. Suppose that $d(x,t)$ is bounded by some known constant Δ due to the boundedness of d_1, *i.e.*, $|d(x,t)| < \Delta$. Note also that the control volumes v_1 and v_2 are always positive and bounded in practical applications. Thus, there must exist some positive constants $\phi_{1min} > 0$ and $\phi_{1max} > 0$ such that $\phi_{1min} < \phi_1 < \phi_{1max}$. Similarly, ϕ_2 is bounded by some constant ϕ_{2min} and ϕ_{2max}, i.e., $\phi_{2min} < \phi_2 < \phi_{2max}$.

It should be noted that the rod displacement x_A of the actuator is not known, thus the control volumes v_1 and v_2 are both unknown. Moreover, the dynamics of the long transmission lines is also not known due to the complicated characteristic of the pipe. Hence, it can be concluded form (12) that ϕ_1 is not known. However, ϕ_1 is bounded according to the above discussion; thus, it is reasonable to assume that ϕ_1 can be modeled by a nominal part plus a uncertain part, i.e., $\phi_1 = \phi_{10} + \Delta\phi_1$, in which ϕ_{10} and $\Delta\phi_1$ are the nominal part and uncertain part of ϕ_1, respectively. Similarly, ϕ_2 can be modeled by $\phi_2 = \phi_{20} + \Delta\phi_2$, in which ϕ_{20} and $\Delta\phi_2$ are the

nominal part and uncertain part of ϕ_2, respectively. Considering the uncertainties of ϕ_1 and ϕ_2, the barrel system (12) can be rewritten as

$$\begin{cases} \dot{\xi}_1 = \xi_2 \\ \dot{\xi}_2 = \xi_3 \\ \dot{\xi}_3 = \phi_{10}u - \phi_{20}(P_1 - P_2) + d_{lump} \\ y = \xi_1 \end{cases} \tag{13}$$

where $d_{lump} = d + \Delta\phi_1 u - \Delta\phi_2(P_1 - P_2)$ is the lumped disturbance. Note that d, $\Delta\phi_1$, $\Delta\phi_2$, u, P_1 and P_2 are all bounded, thus it is reasonable to assume that d_{lump} is bounded by some known positive constant δ, that is, $|d_{lump}| < \delta$.

B. POSITION TRACKING CONTROLLER DESIGN

In this section, the sliding mode technique will be employed to design the position tacking controller of the barrel servo system based on the design model (13). Define the tracking errors as

$$e = \xi_1 - x_d \tag{14}$$

Thus, by using (13), the time derivatives of (14) can be given as

$$\dot{e} = \dot{\xi}_1 - \dot{x}_d = \xi_2 - \dot{x}_d \tag{15a}$$
$$\ddot{e} = \dot{\xi}_2 - \ddot{x}_d = \xi_3 - \ddot{x}_d \tag{15b}$$
$$\dddot{e} = \dot{\xi}_3 - \dddot{x}_d = \phi_{10}u - \phi_{20}(P_1 - P_2) + d_{lump} - \dddot{x}_d \tag{15c}$$

Define the sliding surface as

$$s = k_0 \int_0^t e(\tau)d\tau + k_1 e + k_2 \dot{e} + \ddot{e} \tag{16}$$

where k_0, k_1, k_2 are some positive constants to be designed later, and they are chosen such that the characteristic polynomial $p^3 + k_2 p^2 + k_1 p + k_0$ is Hurwitz. Hence, the position tracking error e will converge to zero exponentially if the sliding variable s is zero.

By using (15), the time derivative of (16) can be given as

$$\begin{aligned} \dot{s} &= k_0 e + k_1 \dot{e} + k_2 \ddot{e} + k_3 \dddot{e} \\ &= k_0 e + k_1 \dot{e} + k_2 \ddot{e} + \phi_{10}u - \phi_{20}(P_1 - P_2) + d_{lump} - \dddot{x}_d \end{aligned} \tag{17}$$

Now, the following theorem can be summarized.

Theorem 1: For the barrel servo system (10) satisfying the assumption 1-2, if the control law is design as

$$u = \frac{1}{\phi_{10}}(-k_0 e - k_1 \dot{e} - k_2 \ddot{e} + \phi_{20}(P_1 - P_2) + \dddot{x}_d) - \frac{1}{\phi_{10}}(k_s s + (\Delta + \eta)sign(s)) \tag{18}$$

where $k_s > 0$ and $\eta > 0$ are controller parameters to be chosen later. Then the sliding variable (16) will converge to zero in finite time. And consequently, the position tracking error (14) will converge to zero exponentially and all signals will be bounded.

Proof: Considering the following positive definite Lyapunov function

$$V_c = \frac{1}{2}s^2 \tag{19}$$

By using (17) and (18), the time derivative of (19) along the system (13) is given as

$$\begin{aligned} \dot{V}_c &= s\dot{s} \\ &= s(k_0 e + k_1 \dot{e} + k_2 \ddot{e} + \phi_{10}u - \phi_{20}(P_1 - P_2) + d_{lump} - \dddot{x}_d) \\ &\le -k_s s^2 + \left|d_{lump}\right| s - \delta\,|s| - \eta\,|s| \\ &\le -2k_s V_c - \sqrt{2}\eta V_c^{1/2} \end{aligned} \tag{20}$$

Thus, there exists a finite time $T > 0$ such that the sling variable s will converge to zero [30]. And consequently, the position tracking error (14) will converge to zero exponentially due to the exponential converge rate of the sliding variable s, and all signals will be bounded due to the boundedness of the practical system states and the desired motion trajectory. The proof is completed.

C. DESIGN OF STATES AND DISTURBANCE OBSERVER WITH ZERO ERRORS

Note that the control law (18) cannot be implemented directly since the system states ξ_2, ξ_3 are not known. However, if the state x_2 and the disturbance d_1 are known exactly, then ξ_2, ξ_3 can be calculated based on (11). Thus, the goal in this section is to estimate x_2 and d_1 with zero estimation errors. In the next step, the linear ESO [25], [26] and the Levant's Differentiator [22] will be combined to simultaneously estimate the unknown state x_2 and the disturbance d_1.

Since only x_2 and d_1 need to be estimated, only the first two equations of (10) are used to design the observer. As in the ESO design, the disturbance d_1 is extended as a new state x_e, i.e., $x_e = d_1$, and its time derivative is defined as $h(t)$, that is, $\dot{x}_e = h(t)$. Note that the time derivative of d_1 is bounded by δ, thus, $h(t)$ is also bounded by δ, i.e., $|h(t)| < \delta$. Thus, it can be obtained that

$$\begin{cases} \dot{x}_1 = x_2 \\ \dot{x}_2 = ax_3 + x_e \\ \dot{x}_e = h(t) \end{cases} \tag{21}$$

To achieve zero estimation errors, the Linear ESO is integrated with the Levant's differentiator [22]. The designed states observer is given as

$$\begin{cases} \dot{\hat{x}}_1 = \hat{x}_2 + 3\omega_0 \tilde{x}_1 + H_3 L^{2/3} sign(\tilde{x}_1)|\tilde{x}_1|^{2/3} \\ \dot{\hat{x}}_2 = a\hat{x}_e + 3\omega_o^2 \tilde{x}_1 + H_2 L^{1/3} sign(\tilde{x}_1)|\tilde{x}_1|^{1/3} \\ \dot{\hat{x}}_e = \omega_o^3 \tilde{x}_1 + H_1 L sign(\tilde{x}_1) \end{cases} \tag{22}$$

where ω_o, L, H_1, H_2, H_3 are positive constants to be chosen later. Let the estimation of $*$ be $\hat{*}$, and the estimation error is defined as $\tilde{*} = * - \hat{*}$. It can be obtained from (21) and (22) that

$$\begin{cases} \dot{\tilde{x}}_1 = \tilde{x}_2 - 3\omega_o \tilde{x}_1 - H_3 L^{2/3} sign(\tilde{x}_1)|\tilde{x}_1|^{2/3} \\ \dot{\tilde{x}}_2 = a\tilde{x}_e - 3\omega_o^2 \tilde{x}_1 - H_2 L^{1/3} sign(\tilde{x}_1)|\tilde{x}_1|^{1/3} \\ \dot{\tilde{x}}_e = h(t) - \omega_o^3 \tilde{x}_1 - H_1 L sign(\tilde{x}_1) \end{cases} \tag{23}$$

which can be written as $\dot{\tilde{x}} = \varphi_1 + \varphi_2$, where

$$\varphi_1 = \begin{bmatrix} -H_3 L^{1/3} sign(\tilde{x}_1)|\tilde{x}_1|^{2/3} + 0.5\tilde{x}_2 \\ -H_2 L^{1/2} sign(\tilde{x}_1)|\tilde{x}_1|^{1/3} + 0.5\tilde{x}_3 \\ -H_1 L sign(\tilde{x}_1) + h(t) \end{bmatrix} \quad (24)$$

$$\varphi_2 = \begin{bmatrix} -3\omega_0 & 0.5 & 0 \\ -3\omega_o^2 & 0 & 0.5 \\ -\omega_o^3 & 0 & 0 \end{bmatrix} \begin{bmatrix} \tilde{x}_1 \\ \tilde{x}_2 \\ \tilde{x}_e \end{bmatrix} = A\tilde{x} \quad (25)$$

in which $A = \begin{bmatrix} -3\omega_0 & 0.5 & 0 \\ -3\omega_o^2 & 0 & 0.5 \\ -\omega_o^3 & 0 & 0 \end{bmatrix}$.

Note that $\dot{\tilde{x}} = \varphi_1$ is finite time stable [22], thus, there must exist some real numbers $0 < \alpha < 1$, $c > 0$ and continuous positive definite function V_1 such that [31]

$$\dot{V}_1 \leq -cV_1^{\alpha} \quad (26)$$

Note also that the matrix A is Hurwitz since $\omega_o > 0$, thus there must exist some symmetric positive definite matrix P such that

$$A^T P + PA = -I_{3\times 3} \quad (27)$$

where $I_{3\times 3}$ is the unit matrix. Define the positive definite Lyapunov function as follows

$$V_2 = \tilde{x}^T P \tilde{x} \quad (28)$$

Since P is a symmetric positive definite matrix, it can be obtained that

$$\frac{V_2}{\lambda_{\max}(P)} \leq \|\tilde{x}\|^2 \leq \frac{V_2}{\lambda_{\min}(P)} \quad (29)$$

The time derivative of (28) using (23) can be given as

$$\begin{aligned} \dot{V}_2 &= \dot{\tilde{x}}^T P\tilde{x} + \tilde{x}^T P\dot{\tilde{x}} \\ &= (A\tilde{x})^T P\tilde{x} + \tilde{x}^T P(A\tilde{x}) \\ &= \tilde{x}^T (A^T P + PA)\tilde{x} \\ &= -\tilde{x}^T \tilde{x} \\ &\leq -\frac{V_2}{\lambda_{\max}(P)} \end{aligned} \quad (30)$$

Thus, the system $\dot{\tilde{x}} = \varphi_2 = A\tilde{x}$ is exponentially stable, i.e., $\tilde{x} \to 0$ as $t \to \infty$. And the converge rate can be tuned effectively by ω_o since the maximum eigenvalue of P is determined by ω_o.

To verify the stability of the proposed observer, define the Lyaponuv function as $V_o = V_1 + V_2$. By using (26) and (30), its time derivative can be given as

$$\dot{V}_o = \dot{V}_1 + \dot{V}_2 \leq -cV_1^{\alpha} - \frac{V_2}{\lambda_{\max}(P)} \leq 0 \quad (31)$$

Thus, V_o together with V_1 and V_2 will converge to zero exponentially. And consequently, the estimation errors will also converge to zero exponentially, that is, $\tilde{x}_i \to 0 (i = 1, 2, e)$ as $t \to \infty$. Note that the states of system (21) are finite, thus, all the signals will be bounded.

Remark 1: The Linear ESO has bounded estimation errors [24]–[26] while the Levant's Differentiator can only estimate the unmeasured states [22]. By combine the advantages of the linear ESO and the Levant's Differentiator, a novel nonlinear ESO is proposed, which can simultaneously estimate the unknown state and disturbance with zero estimation errors.

Remark 2: The parameter ω_o is similar to the observer bandwidth in linear ESO [25], [26], L, H_i $(i = 1, 2, 3)$ are the same as the Levant's differentiator [22], namely, L should be chosen such that $L > \delta$, and $H_1 = 1.1, H_2 = 1.3, H_3 = 3$. General speaking, ω_o should be chosen large enough to attenuate the model uncertainties while L should be chosen such that $L > \delta$. However, too large values may lead to stability issues due to the discretization of the observer and the sample noise. Thus, the selection of the observer parameters should balance the estimation performance and the stability in real applications. A simple but effective method is following the parameter design of linear ESO [25], [26] and the Levant's differentiator [22] simultaneously.

Now, the estimated signals can be used in the controller design, thus the control law (18) can be rewritten as

$$\begin{aligned} u = \frac{1}{\phi_{10}}(-k_0 e - k_1 \dot{e} - k_2 \ddot{e} + \phi_{20}(P_1 - P_2) + \dddot{x}_d) \\ -\frac{1}{\phi_{10}}(k_s s + (\Delta + \eta) sign(s)) \end{aligned} \quad (32)$$

where $e = \hat{\xi}_1 - x_d$, $\dot{e} = \hat{\xi}_2 - \dot{x}_d$, $\ddot{e} = \hat{\xi}_3 - \ddot{x}_d$.

D. STABILITY ANALYSIS OF THE CLOSED LOOP SYSTEM

The proof of the closed loop system stability is similar to the process in the works [20] and [32]. The stability of the closed loop system will be established in the following three steps:

(1) In the first step, the estimation errors (23) converge to zero as shown in section 3.3, i.e., $\tilde{\xi}_1 \to 0$, $\tilde{\xi}_2 \to 0$, $\tilde{\xi}_e \to 0$ as $t \to \infty$. Since the initial condition of the observer are finite and the states of the barrel servo system are bounded according to the assumption 1-2, the estimated signals are also bounded, *i. e.*, $\left|\hat{\xi}_1\right| < \infty$, $\left|\hat{\xi}_2\right| < \infty$, $\left|\hat{\xi}_e\right| < \infty$.

(2) After the converge to zero of the estimation errors of the observer (22), the sliding variable (16) will converge to zero in a finite time T under the control effort of the control law (29). Note that the calculation of the variable s is based on the estimated signals provided by the observer (22).

(3) In the last step, the position tracking error (14) will converge to zero exponentially due to the exponential converge rate of the sliding variable (16). And consequently, the controlled plant (x_1 - x_d) will also converge to zero exponentially.

To further verify the stability of the closed loop system, define the following Lyapunov function

$$V = V_c + V_o = V_c + V_1 + V_2 = \frac{1}{2}s^2 + V_1 + \tilde{x}^T P\tilde{x} \quad (33)$$

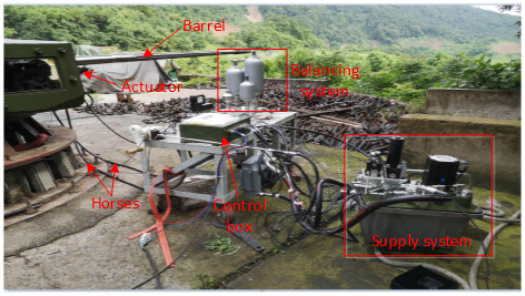

FIGURE 4. The barrel system.

By using (13), (23) and (27), the time derivative of (30) can be given as

$$\begin{aligned}\dot{V} &= s\dot{s} + \dot{V}_1 + \dot{\tilde{x}}^T P\tilde{x} + \tilde{x}^T P\dot{\tilde{x}} \\ &\le -2k_s V_c - \sqrt{2}\eta V_c^{1/2} - cV_1^{\alpha} - \frac{V_2}{\lambda_{\max}(P)} \\ &\le 0 \end{aligned} \tag{34}$$

Thus, the Lyapunov function V together with V_c and V_o will converge to zero exponentially. And consequently, the sliding variable s and the position tracking error e will converge to zero exponentially.

IV. EXPERIMENTAL RESULTS

To evaluate the performance of the proposed controller, an experimental test rig of the barrel servo system had been set up in our laboratory, which is shown in Figure 4. The barrel servo system consists mainly of an electrohydraulic servo system and a hydraulic active balancing system. The electrohydraulic servo system is powered by a fixed displacement pump (5.20 mL/r) which is driven by a servo motor (2.0 Kw). The actuator is a custom-made two-stage single-rod hydraulic cylinder with large effective area ratio (1963.5 mm^2 vs. 326.7 mm^2, stroke length 311.0 mm). The servo valve is a high response rotate direct drive servo valve with the natural frequency of 100 Hz and the rated flow rate of 30 L/min at 7.0 Mpa pressure drop. The pressures at port A and port B of the servo valve are measured via two pressure sensors (25.0 Mpa, ±0.25% FSO). The actuator and the servo valve are connected by hydraulic horses with the internal diameter of 10.0 mm and the length of 2.8 m. The angle position of the barrel is measured via an absolute encoder (resolution ±0.022°). The control algorithms are coded in C program and carried out in a commercial programmable logic controller (667 Mhz). All the signals are measured with the sampling rate of 2.0 ms in the experiments.

The nominal value of ϕ_1 and ϕ_2 are set as 1.0, 0.01, respectively, that is, $\phi_{10} = 1.0$, $\phi_{20} = 0.01$. The parameters of the proposed controller are set as $k_0 = 1.0 \times 10^{-5}$, $k_1 = 0.015$, $k_2 = 1.0 \times 10^{-4}$, $k_s = 1.5$, $k_{sw} = 5.0$. To attenuate the chattering, the sign function sign(s) is replaced by $s/(|s| + \varepsilon)$, where $\varepsilon = 0.15$.

To verify the effectiveness of the proposed controller, it was compared with the PI control with velocity feedforward

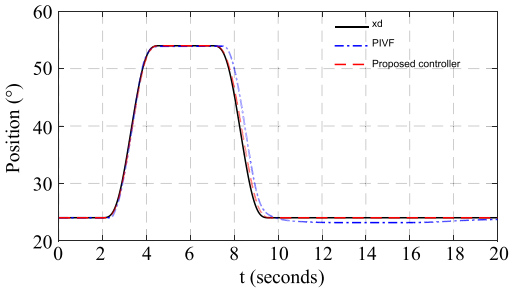

FIGURE 5. Position tracking of PTP motion trajectory.

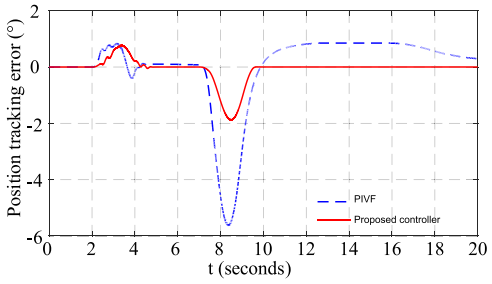

FIGURE 6. Position tracking errors (PTP motion).

(PIVF), which is commonly used in industrial applications. The controller is given as

$$u = k_p e + k_i \int edt + k_v \dot{x}_d$$

where the controller gains k_p, k_i, and k_v were chosen via try-and-error method as $k_p = 0.02$, $k_i = 0.005$ and $k_v = 0.004$.

Three different motion trajectories are tested to evaluate the control performance of the proposed controller and the PIVF.

(1) Point-to-point motion trajectory (PTP): In this case, the classic PTP motion trajectory was tested, the experimental results are shown in Figure 5 – Figure 9.

The position tracking curves and the position tracking errors are shown in Figure5 and Figure 6, respectively. As can be seen, the position tracking errors of the two controllers are almost the same during the ascending motion, the maximum position tracking error of the PIVF is about 0.65 degrees while that of the proposed controller is about 0.63 degrees. However, the steady position tracking error of the PIVF is much larger than that of the proposed controller (0.15 degrees vs. 0.03 degrees). The position tracking error of the proposed controller during the descending motion is about 1.9 degrees, which is about one third of that of the PIVF (about 5.8 degrees). The control performance of the barrel control system is improved by 67.24% in terms of position tracking error during the descending motion. The large position tracking errors during the descending motion is mainly caused by the large effective area ratio (about 6) of the two-stage single-rod actuator. The large effective area ratio leads to very different dynamic characteristic of the barrel servo system from ascending motion to descending motion. Moreover, the steady position tracking error of the proposed

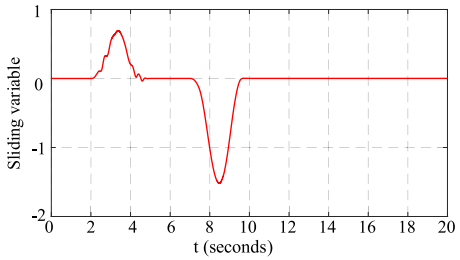

FIGURE 7. Sliding variable (PTP motion).

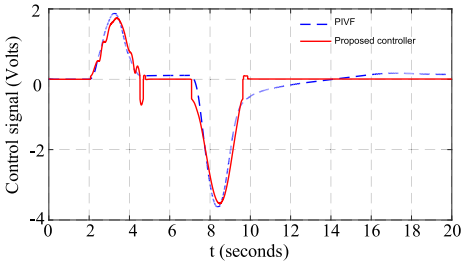

FIGURE 8. Control signals (PTP motion).

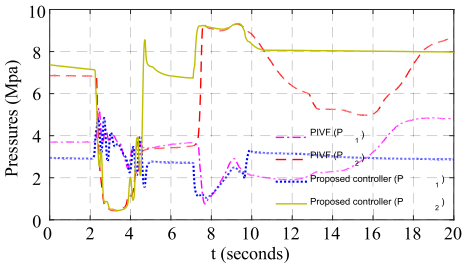

FIGURE 9. Pressures at port A and port B of the servo valve (PTP motion).

controller is still about 0.03 degrees while that of the PIVF is about 0.9 degrees during the descending motion, which is about 30 times of that of the proposed controller.

The sliding variable of the proposed controller and the control signals of the two controllers are depicted in Figure 7 and Figure 8, respectively. As can be seen, no obvious chattering appears in the control signals. The pressures at port A and port B of the servo valve are given in Figure 9.

(2) Sinusoidal motion trajectory: The sinusoidal motion trajectory was tested in this case, i.e.,

$$x_d = 36 + 6\sin(0.5\pi t).$$

The experimental results are shown in Figure 10 – Figure 13.

As can be seen from Figure 10, the position tracking error of the proposed controller is about -1.5 degrees – 0.8 degrees while that of the PIVF is about -2.0 degrees – 1.6 degrees. The position tracking error of the proposed controller is still much smaller than that of the PIVF in this case. The asymmetry of position tracking error is still mainly caused by the large effective area ratio of the actuator.

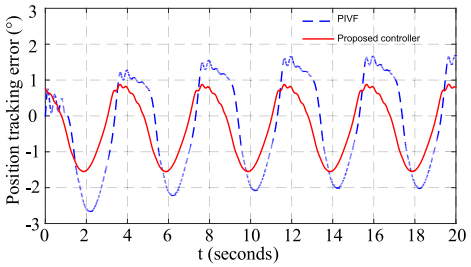

FIGURE 10. Position tracking error (sine).

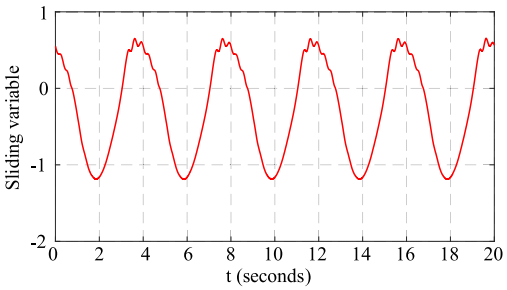

FIGURE 11. Sliding variable (sine).

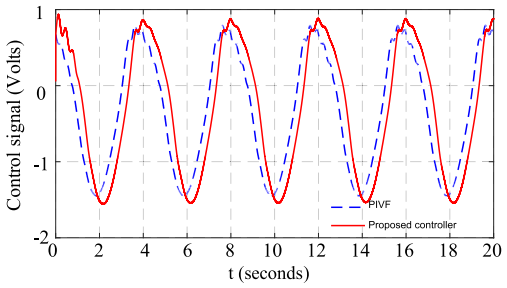

FIGURE 12. Control signals (sine).

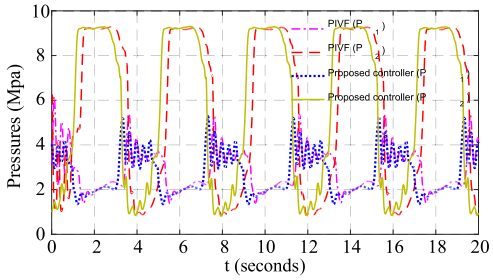

FIGURE 13. Pressures of the two chambers (sine).

The sliding variable of the proposed controller and the control signals of the two controllers are shown in Figure 11 and Figure 12, respectively. Both of the two controller suffer a little chattering under the effort of large control signals, and this is mainly because of the effect of the long transmission lines. This can also be seen form the pressures of the servo valve, which is depicted in Figure 13. Some pressure oscillations appear at the time around the fourth second, the eighth second, the twelfth second, the sixteenth second and

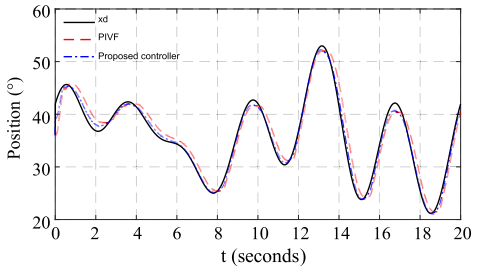

FIGURE 14. Position tracking of multi-frequency sinusoidal motion.

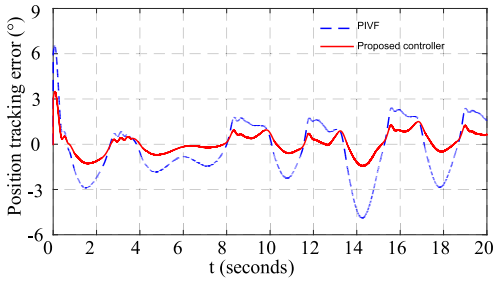

FIGURE 15. Position tracking error of multi-frequency sinusoidal motion.

the twentieth second, which is corresponded to the time at which the chattering appears in the control signals.

(3) sinusoidal motion trajectory with multi-frequency: The sinusoidal-like motion trajectory with multi-frequency was tested in this case, i.e.,

$$x_d = 36 + 6(\sin 0.5\pi t + \cos 0.6\pi t + \sin 0.2\pi t).$$

The experimental results are shown in Figure 14 and Figure 15. As can be seen, the position tracking error of the proposed controller is still much smaller than the PIVF. The other experimental results are not given in this case for the limitation of paper length.

V. CONCLUSIONS

In this paper, the position tracking control of a hydraulic driven barrel system with long transmission lines was addressed. In order to balance the gravitational torques, an active balancing system was designed. The active balancing system is composed of a two-stage hydraulic cylinder and three accumulators. The accumulators were placed in parallel and the gas pressure of each accumulator was carefully designed, thus each of them works mainly at specific barrel angles. Moreover, the active balancing system was totally isolated from the barrel servo system, thus the dynamics of the barrel servo system was significantly simplified. The barrel was driven by another actuator whose structure and placement are the same as that of the active balancing system. Hence, the synchronous of the two hydraulic cylinders are guaranteed physically. In order to use the sliding mode control without back-stepping or multi-surface, the barrel servo system was transformed into the pure integration chain form by defining a set of new state variables. Then a sliding mode controller was designed based on the transformed system to make the barrel angle to track the desired motion trajectories as close as possible in the presence of mode uncertainty and unknown dynamics. Since the transform of the barrel servo system into the pure integration form needs the mechanical disturbance to be known exactly, a nonlinear extended state observer was designed by incorporating the Levant's Differentiator. The designed nonlinear ESO was proven to be of zero estimation errors. Three motion trajectories were tested to evaluate the performances of the proposed controller. Experimental results show that the proposed controller has a much better control performance than the commonly used PI control with velocity feedforward. The pressure signals are needed by the proposed controller. However, the pressure signals are not always available in real application, thus, our future work will focus on the application of the proposed control method on pure output feedback control of EHS.

REFERENCES

[1] D. J. Purdy, "Comparison of balance and out of balance main battle tank armaments," *Shock Vib.*, vol. 8, nos. 3–4, pp. 167–174, 2001.
[2] Q. Gao, Y. Hou, J. Liu, R. Hou, and M. Lv, "An extended state observer based fractional order sliding-mode control for a novel electro-hydraulic servo system with iso-actuation balancing and positioning," *Asian J. Control*, vol. 21, no. 1, pp. 289–301, 2019.
[3] T. Karayumak, "Modeling and stabilization control of a main battle tank," Ph.D. dissertation, Dept. Mech. Eng., Middle East Tech. Univ., Ankara, Turkey, 2011.
[4] C. W. Han, "The robust control and application of artillery position servo system," Ph.D. dissertation, School Mech. Eng., Xi'an Jiaotong Univ., Xi'an, China, 2002.
[5] W. Lee, S. Yoo, S. Nam, K. Kim, and W. K. Chung, "Passivity-based robust compliance control of electro-hydraulic robot manipulators with joint angle limit," *IEEE Robot. Automat. Lett.*, vol. 5, no. 2, pp. 3190–3197, Apr. 2020.
[6] H. Kogler, M. Schöberl, and R. Scheidl, "Passivity-based control of a pulse-width mode operated digital hydraulic drive," *Proc. Inst. Mech. Eng., I, J. Syst. Control Eng.*, vol. 233, no. 6, pp. 656–665, 2018.
[7] M. Fallahi, M. Zareinejad, K. Baghestan, A. Tivay, S. M. Rezaei, and A. Abdullah, "Precise position control of an electro-hydraulic servo system via robust linear approximation," *ISA Trans.*, vol. 80, pp. 503–512, Sep. 2018.
[8] N. D. Manring, L. Muhi, R. C. Fales, V. S. Mehta, J. Kuehn, and J. Peterson, "Using feedback linearization to improve the tracking performance of a linear hydraulic-actuator," *J. Dyn. Syst., Meas., Control*, vol. 140, no. 1, p. 1198, 2018.
[9] D. T. Tran, D. X. Ba, and K. K. Ahn, "Adaptive backstepping sliding mode control for equilibrium position tracking of an electrohydraulic elastic manipulator," *IEEE Trans. Ind. Electron.*, vol. 67, no. 5, pp. 3860–3869, May 2020.
[10] W. Hu, F. Ding, J. Zhang, B. Zhang, M. Zhang, and A. Qin, "Robust adaptive backstepping sliding mode control for motion mode decoupling of two-axle vehicles with active kinetic dynamic suspension systems," *Int. J. Robust Nonlinear Control*, vol. 30, no. 8, pp. 3110–3133, 2020.
[11] A. Mohanty and B. Yao, "Integrated direct/indirect adaptive robust control of hydraulic manipulators with valve deadband," *IEEE/ASME Trans. Mechatronics*, vol. 16, no. 4, pp. 707–715, Aug. 2011.
[12] B. Helian, Z. Chen, and B. Yao, "Precision motion control of a servomotor-pump direct-drive electrohydraulic system with a nonlinear pump flow mapping," *IEEE Trans. Ind. Electron.*, vol. 67, no. 10, pp. 8638–8648, Oct. 2020, doi: 10.1109/TIE.2019.2947803.
[13] M. Won and J. K. Hedrick, "Multiple-surface sliding control of a class of uncertain nonlinear systemsm," *Int. J. Control*, vol. 64, no. 4, pp. 693–706, 1996.
[14] S. K. Pandey, S. L. Patil, D. Ginoya, U. Chaskar, and S. B. Phadke, "Robust control of mismatched buck DC–DC converters by PWM-based sliding mode control schemes," *Control Engineering Practice*, vol. 84, pp. 183–193, Mar. 2019.
[15] M. P. Aghababa and S. Moradi, "Robust adaptive dynamic surface back-stepping tracking control of high-order strict-feedback nonlinear systems via disturbance observer approach," *Int. J. Control*, to be published, doi: 10.1080/00207179.2020.1712478.

[16] J. Zhang, X. Liu, Y. Xia, Z. Zuo, and Y. Wang, "Disturbance observer-based integral sliding-mode control for systems with mismatched disturbances," *IEEE Trans. Ind. Electron.*, vol. 63, no. 11, pp. 7040–7048, Nov. 2016.
[17] J. Yang, S. Li, and X. Yu, "Sliding-mode control for systems with mismatched uncertainties via a disturbance observer," *IEEE Trans. Ind. Electron.*, vol. 60, no. 1, pp. 160–169, Jan. 2013.
[18] X. Yu and O. Kaynak, "Sliding-mode control with soft computing: A survey," *IEEE Trans. Ind. Electron.*, vol. 56, no. 9, pp. 3275–3285, Sep. 2009.
[19] Q. Guo, G. Shi, D. Wang, C. He, J. Hu, and W. Wang, "Iterative learning based output feedback control for electro-hydraulic loading system of a gait simulator," *Mechatronics*, vol. 54, pp. 110–120, Oct. 2018.
[20] J. J. Rath, M. Defoort, H. R. Karimi, and K. C. Veluvolu, "Output feedback active suspension control with higher order terminal sliding mode," *IEEE Trans. Ind. Electron.*, vol. 64, no. 2, pp. 1392–1403, Feb. 2017.
[21] J. Na, Y. Li, Y. Huang, G. Gao, and Q. Chen, "Output feedback control of uncertain hydraulic servo systems," *IEEE Trans. Ind. Electron.*, vol. 67, no. 1, pp. 490–500, Jan. 2020.
[22] A. Levant, "Higher-order sliding modes, differentiation and output-feedback control," *Int. J. Control*, vol. 76, nos. 9–10, pp. 924–941, Jan. 2003.
[23] J. Yao, Z. Jiao, and D. Ma, "Extended-State-Observer-Based output feedback nonlinear robust control of hydraulic systems with backstepping," *IEEE Trans. Ind. Electron.*, vol. 61, no. 11, pp. 6285–6293, Nov. 2014.
[24] G. Yang and J. Yao, "Output feedback control of electro-hydraulic servo actuators with matched and mismatched disturbances rejection," *J. Franklin Inst.*, vol. 356, no. 16, pp. 9152–9179, Nov. 2019.
[25] B.-Z. Guo and Z.-L. Zhao, "On the convergence of an extended state observer for nonlinear systems with uncertainty," *Syst. Control Lett.*, vol. 60, no. 6, pp. 420–430, Jun. 2011.
[26] Q. Zheng, L. Q. Gaol, and Z. Gao, "On stability analysis of active disturbance rejection control for nonlinear time-varying plants with unknown dynamics," in *Proc. 46th IEEE Conf. Decis. Control*, Dec. 2007, pp. 3501–3506.
[27] R. Madoński and P. Herman, "Survey on methods of increasing the efficiency of extended state disturbance observers," *ISA Trans.*, vol. 56, pp. 18–27, May 2015.
[28] K. Butt and N. Sepehri, "A nonlinear integral sliding surface to improve the transient response of a force-controlled pneumatic actuator with long transmission lines," *J. Dyn. Syst., Meas., Control*, vol. 141, no. 12, Dec. 2019, Art. no. 121012.
[29] E. Richer and Y. Hurmuzlu, "A high performance pneumatic force actuator system: Part I—Nonlinear mathematical model," *J. Dyn. Syst., Meas., Control*, vol. 122, no. 3, pp. 416–425, 2000.
[30] Z. Zuo and L. Tie, "Distributed robust finite-time nonlinear consensus protocols for multi-agent systems," *Int. J. Syst. Sci.*, vol. 47, no. 6, pp. 1366–1375, Apr. 2016, doi: 10.1080/00207721.2014.925608.
[31] S. P. Bhat and D. S. Bernstein, "Geometric homogeneity with applications to finite-time stability," *Math. Control, Signals, Syst.*, vol. 17, no. 2, pp. 101–127, Jun. 2005.
[32] Q. Guo, Y. Zhang, B. G. Celler, and S. W. Su, "Backstepping control of electro-hydraulic system based on Extended-State-Observer with plant dynamics largely unknown," *IEEE Trans. Ind. Electron.*, vol. 63, no. 11, pp. 6909–6920, Nov. 2016.